scientific reports

Check for updates

OPEN

WNT inhibition activates interferon stimulated gene expression by alleviating epigenetic repression of endogenous retroviruses

Courtney M. Williams[1]✉, Jessica Harper Calderon[1], Varenka Rodriguez DiBlasi[2], Louis Jinrui Liu[2], Samer Nuwayhid[1], Hannah Cevasco[1], Wei Wang[2], Rekha Soni[3], Christina Adler[3], David D'Ambrosio[4], Namita T. Gupta[2] & Christopher Daly[1]

As the use of immune checkpoint inhibitors for the treatment of cancer has expanded, convincing data have emerged correlating active WNT signaling with resistance to immunotherapies. To identify mechanisms through which WNT signaling limits anti-tumor immunity, we examined the response to WNT inhibition in a variety of human cancer cell lines that harbor distinct WNT pathway mutations. Our data show that inhibition of WNT signaling leads to activation of the TBK1/IRF3 dsRNA-sensing pathway and expression of interferon-stimulated genes (ISGs), independently of IFN/JAK/STAT signaling. Mechanistically, we show that WNT inhibition leads to increased chromatin accessibility at genomic loci harboring endogenous retroviruses (ERVs), resulting in ERV re-expression and activation of the dsRNA response. Increased ISG expression following WNT inhibition does not involve decreased MAP kinase signaling and therefore differs from reports documenting ISG induction in response to inhibition of other oncogenic pathways. Given the variety of tumor cell lines and WNT pathway mutations examined, these data suggest a mechanism by which WNT may drive immune evasion and several therapeutic avenues to reverse it, including tumor-targeted type 1 interferon stimulation and/or epigenetic therapies.

Keywords WNT signaling, Immunotherapy, Immune checkpoint inhibition, Interferon, Interferon Simulated Genes (ISG), Endogenous Retrovirus (ERV), pancreatic cancer, dsRNA

Despite the remarkable success of immune checkpoint inhibition (ICI) for the treatment of cancer, a significant portion of patients do not respond to these therapies[1]. Tumor types that show particularly low response rates to ICI include pancreatic, prostate, and colorectal cancers. Poor responsiveness can be due to tumor cell-intrinsic factors including low tumor mutation burden, reduced antigen processing and presentation, upregulation of factors that suppress killing by T cells (ex PD-L1), and recruitment of immunosuppressive cells. However, while understood in broad strokes, the molecular mechanisms that promote immune evasion and resistance to ICI are not fully characterized.

Numerous studies have correlated high WNT signaling with poor responsiveness to ICI in a broad range of tumor types[2–6]. These studies show that high WNT signaling correlates with a 'cold' or non-T-cell inflamed gene signature, a state marked by the absence of tumor-infiltrating immune cells. Despite this robust correlation, the mechanism(s) by which WNT signaling promotes immune evasion, and how to counteract it, are poorly understood. The transcription factor MYC, whose expression is induced by WNT signaling, drives expression of CD47 and CD274 (PD-L1), which promote immune evasion by dampening the activity of cytotoxic T cells and other immune cells[7]. However, the precise role of MYC in WNT-driven immune evasion remains to be fully defined since MYC is broadly expressed and induces transcription of a myriad of genes.

The most well-characterized mechanism by which WNT signaling can promote immune evasion was identified using a genetically engineered mouse model harboring mutations in *Braf*, *Ctnnb1*, and *Pten*. Spranger et al. found that WNT drives expression of ATF3, which in turn represses expression of CCL4 and the recruitment

[1]Department of Oncology & Immune-Oncology, Regeneron Pharmaceuticals Inc, Tarrytown, NY, USA. [2]Molecular Profiling & Data Science, Regeneron Pharmaceuticals Inc, Tarrytown, NY, USA. [3]Molecular Profiling Core, Regeneron Pharmaceuticals Inc, Tarrytown, NY, USA. [4]DNA Core, Regeneron Pharmaceuticals Inc, Tarrytown, NY, USA. ✉email: courtney.williams@regeneron.com

of dendritic cells to tumors[8]. Other groups have confirmed the connection between WNT activation, *ATF3* expression, and *CCL4* repression in some human cancer cell lines[6] or have observed a correlation in human tumors[5]. However, given the many genes controlled by WNT and the wide variety of tumor types that fail to respond to ICI, it is unlikely that there is a single mechanism through which WNT signaling limits anti-tumor immunity[1,9].

The WNT signaling pathway is evolutionarily conserved, with critical roles in development and tissue function[10]. In cancer, WNT signaling is activated in multiple tumor types through a variety of mechanisms including loss of function mutations (APC, RNF43), gain of function mutations (CTNNB1), and receptor/ligand overexpression (FZDs, WNTs, RSPOs). Given the ubiquitous expression of WNT receptors and ligands, even tumors without activating mutations in WNT pathway components may have active WNT signaling that modulates anti-tumor immunity.

In this study, we have identified a novel mechanism whereby WNT signaling inhibits the expression of type I interferon-stimulated genes (ISGs) by driving expression of epigenetic repressors that function to silence endogenous retrovirus (ERV) expression. Blockade of WNT signaling thereby leads to re-expression of ERVs and a 'viral mimicry' response which activates ISG expression in a manner independent of type I IFN/JAK/STAT signaling. This response to WNT pathway inhibition is independent of the type of WNT-activating mutation and is observed in a variety of human cancer cell lines, suggesting it may account for the broad association of WNT activation with lack of response to ICI. Our data suggest several mechanisms by which WNT may drive immune evasion and therapeutic avenues to reverse it, including stimulation of type 1 interferon signaling and/or epigenetic therapy.

Results

WNT signaling suppresses the expression of interferon-stimulated genes in cancer cells

To identify potential mechanisms that account for WNT-driven tumor immune evasion, we identified gene expression changes occurring in response to WNT pathway inhibition. We employed three pancreatic cancer cell lines (HPAF-II, AsPc-1, and PaTu8988S) that harbor loss of function mutations in the E3 ubiquitin ligase RNF43, which functions to inhibit ligand-dependent WNT signaling by promoting degradation of FZD receptors. These RNF43 mutant cell lines exhibit active, ligand-dependent WNT signaling. Cells were treated with the porcupine inhibitors ETC-159 or Lgk974 (which block palmitoylation and secretion of WNT ligands) for 24 h and RNA-seq was performed. Gene set enrichment analysis (GSEA) of the RNA-seq data revealed the expected downregulation of genes involved in cell cycle progression (Fig. 1a, Supplemental Fig. 1) and of WNT target genes (including *AXIN2* and *MYC*), confirming effective inhibition of WNT signaling (Supplemental Fig. 2). Interestingly, GSEA also showed significant upregulation of ISGs as well as cytokines in all cell lines (Fig. 1a, Supplemental Figs. 1 and 2). Quantitative PCR and Western blot analysis of HPAF-II cells treated with Lgk974 for 48 h confirmed the downregulation of WNT target genes (Fig. 1b and c) and the induction of ISG expression (Fig. 1d and e). The upregulation of ISGs in response to WNT inhibition is notable since interferon signaling plays a complicated and critical role in response to immunotherapy and is known to upregulate antigen processing and presentation[11].

To confirm that the effects of porcupine inhibitors on ISG expression are due to WNT pathway blockade, siRNA was used to knockdown *CTNNB1*, also resulting in increased ISG expression (Fig. 2a, b). Consistent with this finding, we also show that the effects of porcupine inhibition can be reversed by activation of the WNT pathway with exogenous ligand (WNT3A plus RSPO2) (Fig. 2c, d). Thus, the effects of the porcupine inhibitors on ISG expression clearly reflect the on-target action of these agents on the WNT signaling pathway.

Given that HPAF-II, AsPc-1, and PaTu8988S cells all harbor RNF43 mutations that enhance ligand-dependent WNT signaling, cell lines with a variety of other WNT pathway genetic alterations were tested for induction of ISGs following inhibition of WNT signaling. Using *CTNNB1* siRNA to inhibit the WNT pathway in cells with ligand-independent signaling and Lgk974 to inhibit the WNT pathway in cells with ligand-dependent signaling, we found that cell lines harboring CTNNB1 activating mutations (HepG2, LIM1215), APC inactivating mutations (T84, KATOIII), or RSPO3-fusion (JHOM2B) all show induction of ISGs upon WNT inhibition (Fig. 3a). Notably, the pattern of ISG induction in the different cell lines is distinct (e.g., *OAS1* is not induced in HepG2 cells), suggesting that expression of ISGs is cell-context dependent. These findings indicate that cancer cells from several lineages, harboring a variety of WNT pathway genetic alterations, respond to inhibition of WNT signaling by increasing the expression of ISGs.

Consistent with our observation that activation of WNT signaling by distinct genetic mechanisms results in suppression of ISG expression, we show that activation of the WNT pathway by addition of WNT3A and RSPO3 to cancer cells that lack WNT pathway alterations (J82, CAL27) results in significant downregulation of ISG expression (Fig. 3b). Thus, activation of WNT signaling in cancer cells by genetic alteration of pathway components or by exogenous ligand results in decreased expression of ISGs.

To determine if elevated WNT signaling is also associated with decreased expression of ISGs in human tumors, previously published data from resectable hepatocellular carcinomas (HCC) treated with cemiplimab were re-analyzed[12]. Using this small sample, we designated tumors as "WNT low" versus "WNT high" based on the expression of genes in the Omics WNT Pathway gene list. Tumors were then clustered according to WNT activity, and a subset of ISGs were analyzed (Supplemental Fig. 3). To quantify differences in ISG expression between the WNT high and WNT low tumors, we defined a list of interferon-stimulated genes (ISGs) to generate a signature to score: *IRF6*, *IFIT5*, *IFIT1*, *GBP3*, *DDX58*, *IFIT2*, *IFIT3*, *IFIH1*, *HLA-E*, *HLA-F*, *OAS1*, *OAS2*, *IRF9*, *OASL*, *GBP4*, *IRF1*, *ISG20*, *GBP2*, *IRF7*, and *ISG15* (Supplemental Fig. 3b). As seen in Fig. 3c, the ISG signature score for "WNT high" tumors is lower than that for "WNT low" tumors, and this different correlates with the presence of tumor-infiltrating lymphocytes (TILs) and responsiveness to PD-1 inhibition (Supplemental Fig. 3a, b). While this dataset is made up of a small number of HCC tumor samples, the correlative analysis is consistent

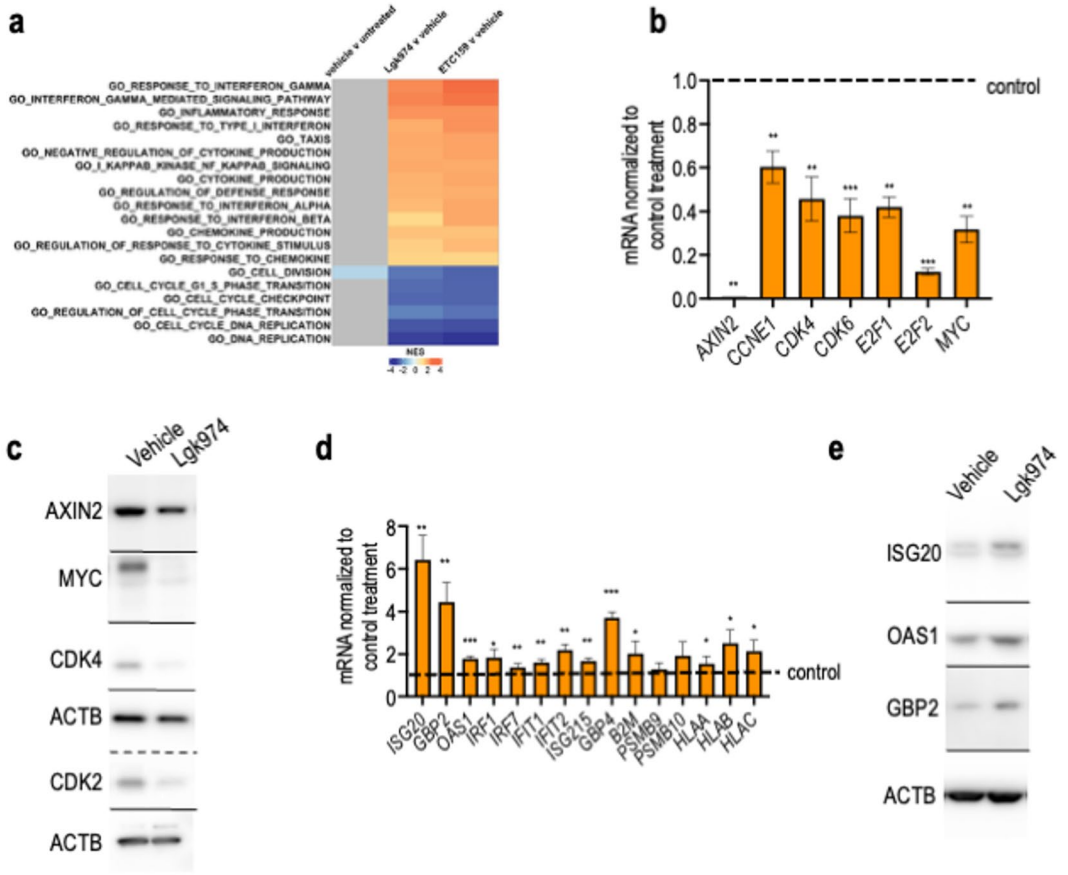

Fig. 1. WNT signaling in pancreatic cancer cells modulates the expression of cell cycle regulators and interferon-stimulated genes. (**a**) HPAF-II cells were treated for 24 h with the porcupine inhibitors Lgk974 or ETC-159 and subjected to RNA-seq and gene set enrichment analysis. The heatmap shows the normalized enrichment scores (NES) for the Gene Ontology (GO) terms indicated. (**b**) Quantitative PCR data showing normalized mRNA levels of WNT target genes in HPAF-II cells treated with Lgk974 for 48 h. The mRNA levels in the vehicle-treated control cells were assigned a value of 1 (dashed line on graph). Error bars show SD, $n = 3$. $^{*}P < 0.05$, $^{**}P < 0.01$, $^{***}P < 0.001$ and $^{****}P < 0.0001$ versus control, multiple unpaired t-tests. (**c**) Western blot of WNT target genes from HPAF-II cells treated with Lgk974 for 48 h. (**d**) Quantitative PCR data showing normalized mRNA levels of select ISGs in HPAF-II cells treated with Lgk974 for 48 h. The mRNA levels in the vehicle-treated control cells were assigned a value of 1 (dashed line on graph). Error bars show SD, $n = 3$. $^{*}P < 0.05$, $^{**}P < 0.01$, $^{***}P < 0.001$ versus control multiple unpaired t-tests. (**e**) Western blot of interferon-stimulated genes from HPAF-II cells treated with Lgk974 for 48 h.

with our findings with human cell lines in vitro, that WNT pathway signaling suppresses ISG expression in human tumors.

WNT inhibition induces ISG expression through activation of the dsRNA response pathway

Expression of ISGs is induced by type-1 Interferons (a/b), which signal through a heterodimeric receptor (IFNAR1/IFNAR2) to activate the kinases JAK1 and TYK2 and the transcription factors STAT1 and STAT2. Although HPAF-II cells respond to exogenous type-I interferon with activation of STAT1 and induction of ISG expression (Fig. 4a, Supplemental Fig. 4a), RNA-seq and quantitative PCR show no significant induction of interferon ligands upon WNT inhibition, save for a minor induction of *IFNE* (data not shown). These data suggest that ligand-dependent activation of IFNAR1/IFNAR2 is not responsible for the induction of ISGs in response to WNT inhibition.

To further test this hypothesis, HPAF-II cells were treated with Lgk974 alone or in the presence of an IFNAR1-blocking antibody or the JAK inhibitor ruxolitinib. While both the IFNAR1-blocking antibody and ruxolitinib inhibited STAT1 phosphorylation in response to exogenous IFNA (Fig. 4a), neither agent blocked induction of ISGs in response to WNT pathway inhibition (Fig. 4b). After 48 h of IFN treatment there is a modest decrease in expression of WNT target genes (Supplemental Fig. 4b); inhibition of WNT pathway activation by IFNs has been previously reported[13]. These data indicate that the induction of ISG expression following inhibition of WNT signaling is not dependent on activation of JAK/STAT signaling by interferons.

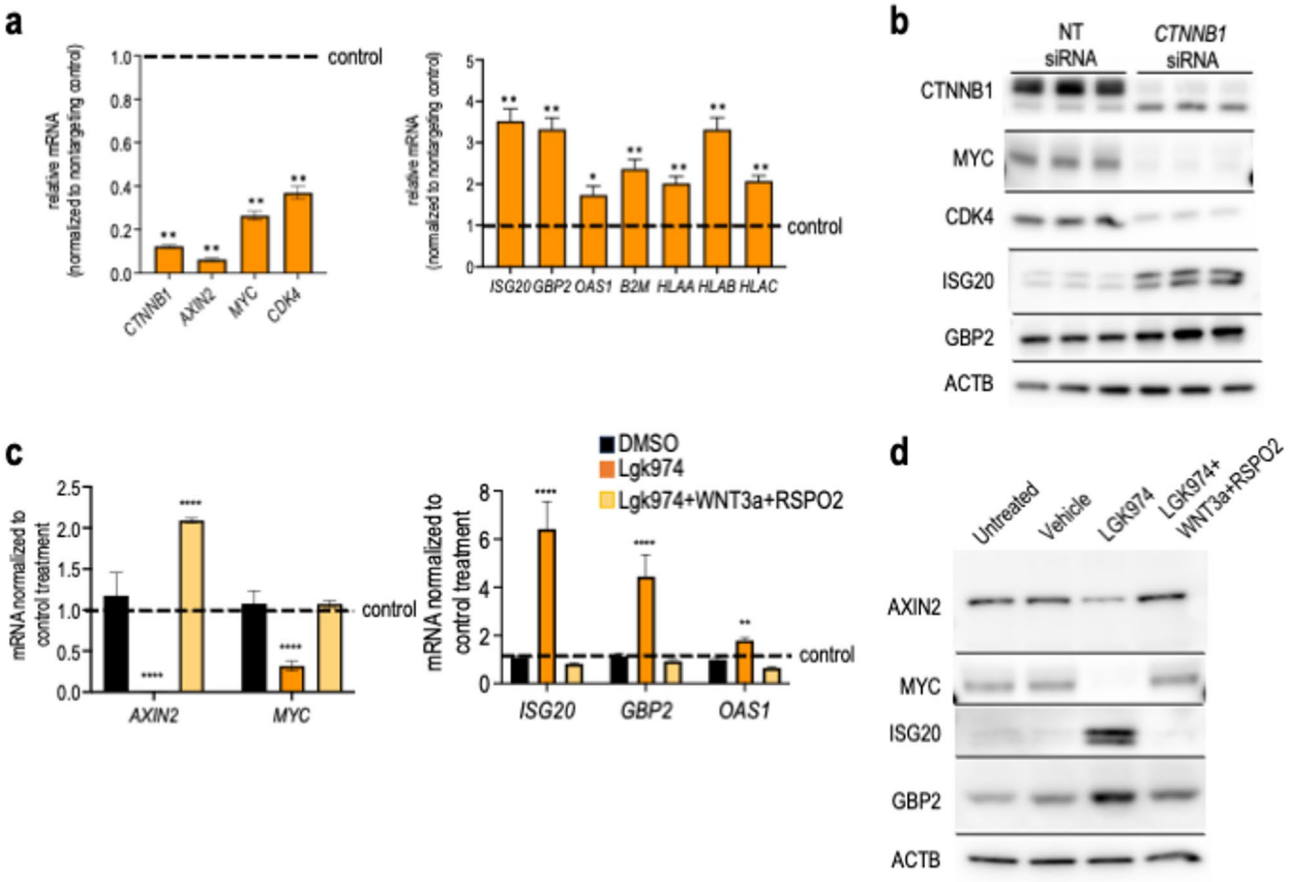

Fig. 2. WNT signaling is necessary and sufficient to suppress expression of ISGs in pancreatic cancer cells. (**a**) Quantitative PCR data showing normalized mRNA levels of WNT target genes and interferon-stimulated genes (ISGs) in HPAF-II cells treated with CTNNB1 siRNA for 48 h. The mRNA levels in the non-targeting control treated cells were assigned a value of 1 (dashed line on graph), $n = 3$. (**b**) Western blot of WNT target genes and ISGs from HPAF-II cells treated as in a. (**c**) Quantitative PCR data showing normalized mRNA levels of WNT target genes and select ISGs in HPAF-II cells treated with Lgk974 alone, or with exogenous WNT3a and RSPO2 for 48 h. The mRNA levels in the vehicle-treated control cells were assigned a value of 1 (dashed line on graph), $n = 3$. (**d**) Western blot from HPAF-II cells treated as in c. (Two-way ANOVA with Tukey's multiple comparison test versus control; * < 0.05, ** < 0.01, *** < 0.001, **** < 0.0001).

Expression of ISGs can also be triggered by ligand-independent, intracellular mechanisms, namely the detection of double-stranded RNA (dsRNA) or double-stranded DNA (dsDNA) by pattern recognition receptors (PRRs) which stimulate ISG expression in a TBK1/IRF3-dependent manner. The dsRNA sensors MDA5 (IFIH1) and RIGI (DDX58) bind viral dsRNA in the cytosol triggering the formation of MAVS aggregates and activation of the kinase TBK1, which in turn phosphorylates and activates the transcription factor IRF3. Similarly, cytosolic dsDNA activates the TBK1/IRF3 pathway and ISG expression via cGAS/STING. Further, a previous report implicates CTNNB1 interaction with IRF3 as a mechanism by which WNT could negatively regulate innate immunity, but that report was specifically in the context of viral infection[14].

To determine if WNT inhibition activates these PRR pathways in cancer cells, HPAF-II cells were treated with *CTNNB1* siRNA for 24 h and Western blotting performed to assess phosphorylation of TBK1 and IRF3. As shown in Fig. 4c, WNT inhibition triggers phosphorylation of TBK1 and IRF3, similar to treatment with dsRNA mimic poly (I: C) (Supplemental Fig. 4c). These data implicate dsRNA/dsDNA and PRRs in the induction of ISG expression following WNT pathway inhibition.

To distinguish between the dsRNA and dsDNA sensing pathways, siRNA was used to knock down the PRRs *STING* (cytosolic dsDNA), *RIGI* and *MDA5* (cytosolic dsRNA), or *TLR3* (endosomal dsRNA). Knockdown of *STING* failed to block Lgk974 induction of ISGs (Fig. 4d), despite almost complete depletion of STING protein. Knockdown of *TLR3* similarly had no effect on ISG induction by Lgk974 (data not shown). In contrast, simultaneous knockdown of *RIGI* and *MDA5* significantly reduced the induction of ISGs following Lgk974 treatment (Fig. 4e, Supplemental Fig. 4d). *RIGI/MDA5* knockdown also reduced baseline expression of ISGs in control cells treated with vehicle alone (Fig. 4e), suggesting that the weak basal ISG expression observed in the presence of active WNT signaling is also dependent on dsRNA sensing. Taken together, these results indicate

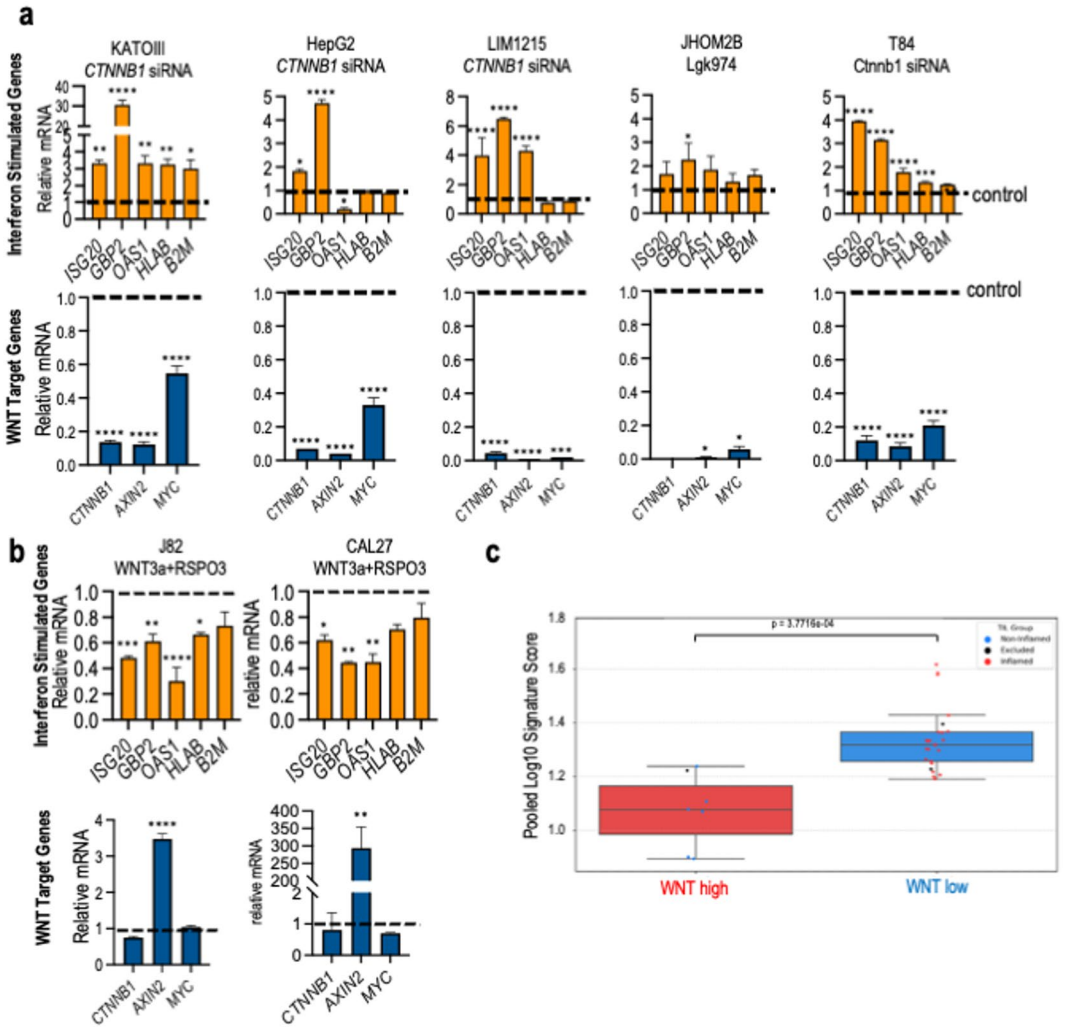

Fig. 3. WNT signaling broadly regulates ISG expression in cancer cells. (**a**) Quantitative PCR data showing normalized mRNA levels of ISGs (top) and WNT target genes (bottom) in the indicated cancer cell lines treated with either Lgk974 or *CTNNB1* siRNA to inhibit WNT signaling. The mRNA levels in the non-targeting siRNA treated control cells or the vehicle-treated control cells (for Lgk974 treatment) were assigned a value of 1 (dashed lines on graphs) ($n = 3$ for JHOM2B, HepG2 KATOIII; $n = 2$ for T84, LIM1215). (**b**) Quantitative PCR data showing normalized mRNA levels of ISGs (top) and WNT target genes (bottom) in J82 and CAL27 cancer cells treated with WNT3a and RSPO3 to activate WNT signaling. The mRNA levels in untreated control cells were assigned a value of 1 (dashed lines on graphs), $n = 3$. (Two-way ANOVA with Fisher's least significant difference test versus control; * < 0.05, ** < 0.01, *** < 0.001, **** < 0.0001) (**c**) Box plot comparing signature scores between 'WNT high' and 'WNT low' samples in resected hepatocellular carcinoma samples profiled in[12]. Statistical significance was assessed using the Mann-Whitney test.

that the dsRNA sensors RIGI and MDA5 are necessary for WNT inhibition to trigger expression of ISGs in WNT mutant HPAF-II cells.

Decreased MYC expression is not sufficient to induce ISG expression following inhibition of WNT signaling

Several groups have reported that MYC, along with its binding partner MIZ1, binds the promoters of ISGs to repress their expression, potentially suppressing innate immunity and allowing tumor immune evasion[15–17]. Given these published findings, and the marked reduction of MYC expression that we observe following inhibition of WNT signaling, we tested if *MYC* knockdown is sufficient to induce ISG expression. As shown in Fig. 5a, *MYC* knockdown alone did not induce ISGs in HPAF-II cells, indicating that in these cells ISG expression requires more than loss of purported MYC-mediated repression at ISG promoters. Additionally, HPAF-II cells have very low levels of the MYC co-repressor MIZ1 (data not shown), which may account for the apparent lack of MYC-mediated ISG repression in these cells. Additional cell lines (LIM1215, PaTu8988S, AsPc-1) were tested to compare the *MYC* versus *CTNNB1* knock-down. As seen in Supplemental Fig. 5, these additional cell lines,

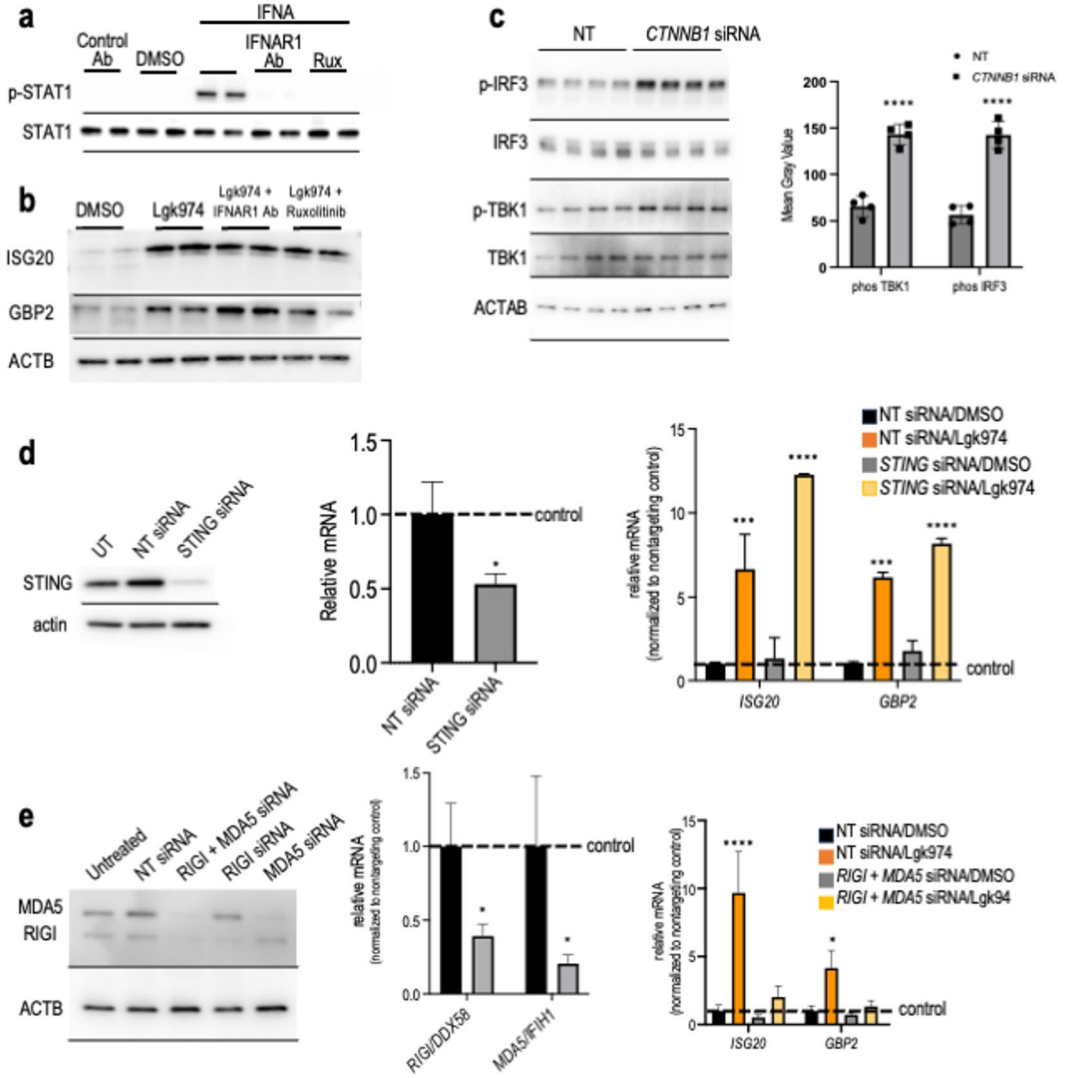

Fig. 4. Inhibition of WNT signaling results in increased ISG expression via activation of the dsRNA sensing pathway. (**a**) Western blot from HPAF-II cells treated with IFNa2B alone or in the presence of ruxolitinib or IFNAR1 blocking antibody for 1 h. (**b**) Western blot from HPAF-II cells treated with Lgk974 alone or in combination with ruxolitinib or IFNAR1 blocking antibody for 48 h. (**c**) Western blot from HPAF-II cells treated with non-targeting (NT) or *CTNNB1* siRNA for 48 h and ImageJ quantification of bands normalized to total IRF3 or TBK1. (**d**) Western blot and quantitative PCR from HPAF-II cells treated with NT control or *STING* siRNA alone or in combination with Lgk974 for 48 h. The mRNA levels in control cells treated with NT siRNA/vehicle control were assigned a value of 1 (dashed line on graph). (**e**) Western blot and quantitative PCR analysis of HPAF-II cells treated with NT siRNA or siRNA targeting *RIGI* and/or *MDA5* alone or in combination with Lgk974. The mRNA levels in control cells treated with NT siRNA/vehicle control were assigned a value of 1 (dashed line on graph). (Blot quantification and ISGs, Two-way ANOVA with Fisher's least significant difference test versus control; siRNA knock down, unpaired t-test * < 0.05, ** < 0.01, *** < 0.001, **** < 0.0001) $n = 3$.

with active WNT signaling, show more robust ISG induction with *CTNNB1* knockdown compared to *MYC* knockdown for the panel of ISGs examined.

In contrast to HPAF-II and other WNT activated cell lines, in the BT-549 breast cancer cell line used by Zimmerli et al., *MYC* knockdown is sufficient to induce expression of several ISGs, while *CTNNB1* knockdown is not (Fig. 5 b). The most likely explanation for the lack of effect of *CTNNB1* knockdown on ISG expression is that the WNT pathway is not constitutively active in these cells, consistent with the absence of WNT pathway activating mutations[18]. Thus, while MYC can directly repress ISG expression in some cell lines (e.g. BT-549), our data indicate that downregulation of MYC is not sufficient for induction of ISG expression in the panel of WNT-driven cancer cell lines examined.

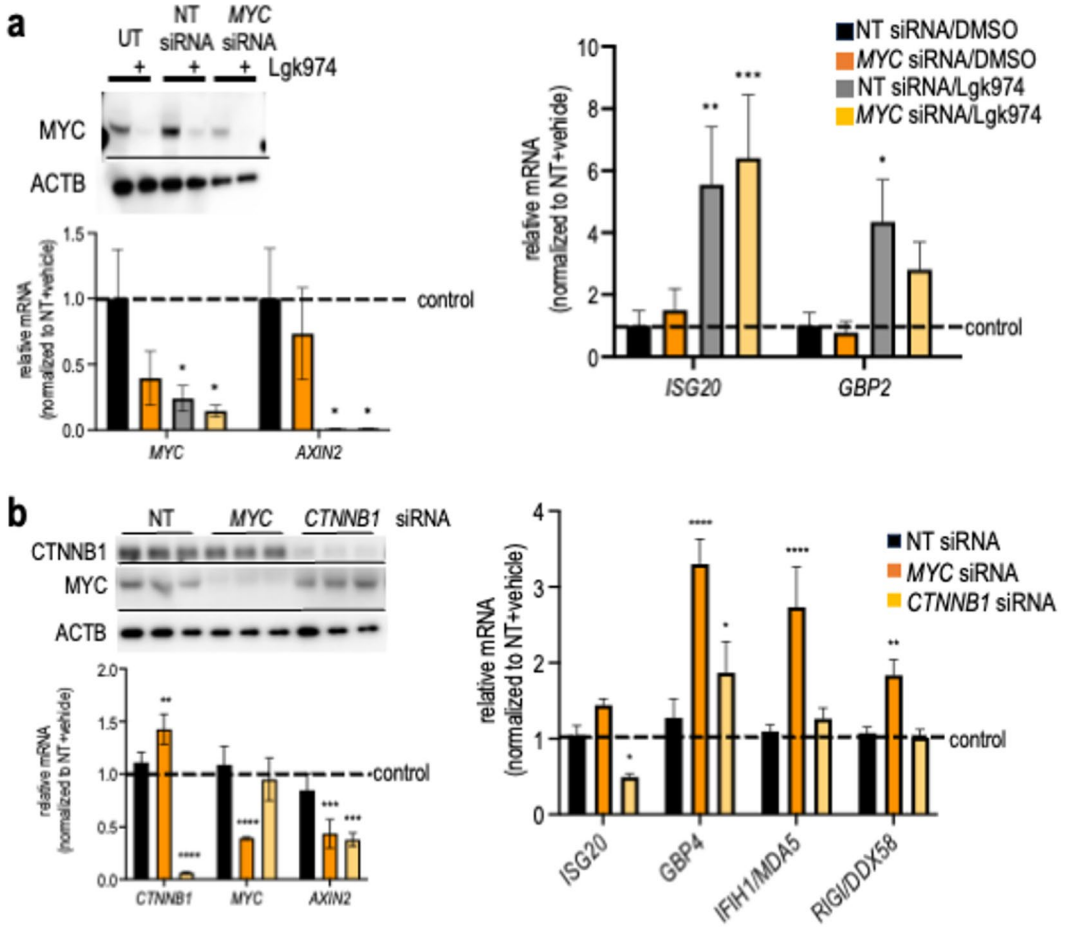

Fig. 5. Decreased MYC expression is not sufficient to induce ISG expression following inhibition of WNT signaling. (**a**) Western blot and quantitative PCR analysis of WNT target genes and ISGs from HPAF-II cells treated with non-targeting (NT) or *MYC* siRNA alone or in combination with Lgk974 for 48 h. The mRNA levels in control cells treated with NT siRNA/vehicle control were assigned a value of 1 (dashed lines on graphs). (**b**) Western blot and quantitative PCR analysis of WNT target genes and ISGs from BT-549 cells treated for 48 h with non-targeting, *MYC* or *CTNNB1* siRNA. The mRNA levels in control cells treated with NT siRNA/vehicle control were assigned a value of 1 (dashed line on graphs). (Two-way ANOVA with Fisher's least significant difference test versus control; * < 0.05, ** < 0.01, *** < 0.001, **** < 0.0001) $n = 3$.

Inhibition of WNT signaling leads to decreased expression of epigenetic repressors and to increased expression of endogenous retroviruses

The term viral mimicry describes the phenomenon whereby aberrant re-expression of endogenous retroviruses (ERVs) triggers formation of dsRNA (via bidirectional transcription from long terminal repeats) and an intracellular antiviral response leading to induction of type-I interferon and ISG expression. Viral mimicry can be triggered by inhibition of epigenetic regulators (e.g., DNMT1, EZH2, KDM1A) that suppress gene expression (including ERVs)[19,20,21]. Since ISGs are involved in a variety of immunostimulatory processes, viral mimicry is actively being explored as a potential mechanism to sensitize tumors to immunotherapies.

WNT inhibition via *CTNNB1* siRNA or Lgk974 treatment results in decreased expression of mRNA and protein levels of several epigenetic repressors including DNMT1, KDM1A, and EZH2 in multiple cancer cell lines (Fig. 6a, b, Supplemental Fig. 6). We hypothesized that loss of epigenetic repression leads to increased chromatin accessibility at ERV loci and ERV re-expression. To explore this possibility, we performed Assay for Transposase-Accessible Chromatin with Sequencing (ATAC-Seq) on HPAF-II cells treated with Lgk974 for 24 and 48 h to identify alterations in chromatin structure. While WNT inhibition results in decreased expression of epigenetic repressors, the overall effect of Lgk974 treatment was to decrease chromatin accessibility genome-wide, including at WNT target gene loci (Supplemental Fig. 7a, b). This finding is in keeping with the role of WNT signaling in maintenance of cell stemness[22,23]. However, despite the overall decrease in chromatin accessibility following WNT inhibition, ATAC-seq revealed a greater than two-fold enrichment of transposase-accessible peaks within putative ERVs in Lgk974 treated cells (Supplemental Fig. 7b). Figure 6c shows a heatmap depicting the number of transposon insertion events at seven differentially accessible ERV-containing regions identified by ATAC-seq. The position of the insertion is mapped relative to transcriptional start and end sites of the nearest gene. Comparing vehicle control treatment to Lgk974 treatment shows a clear increase in accessibility for these

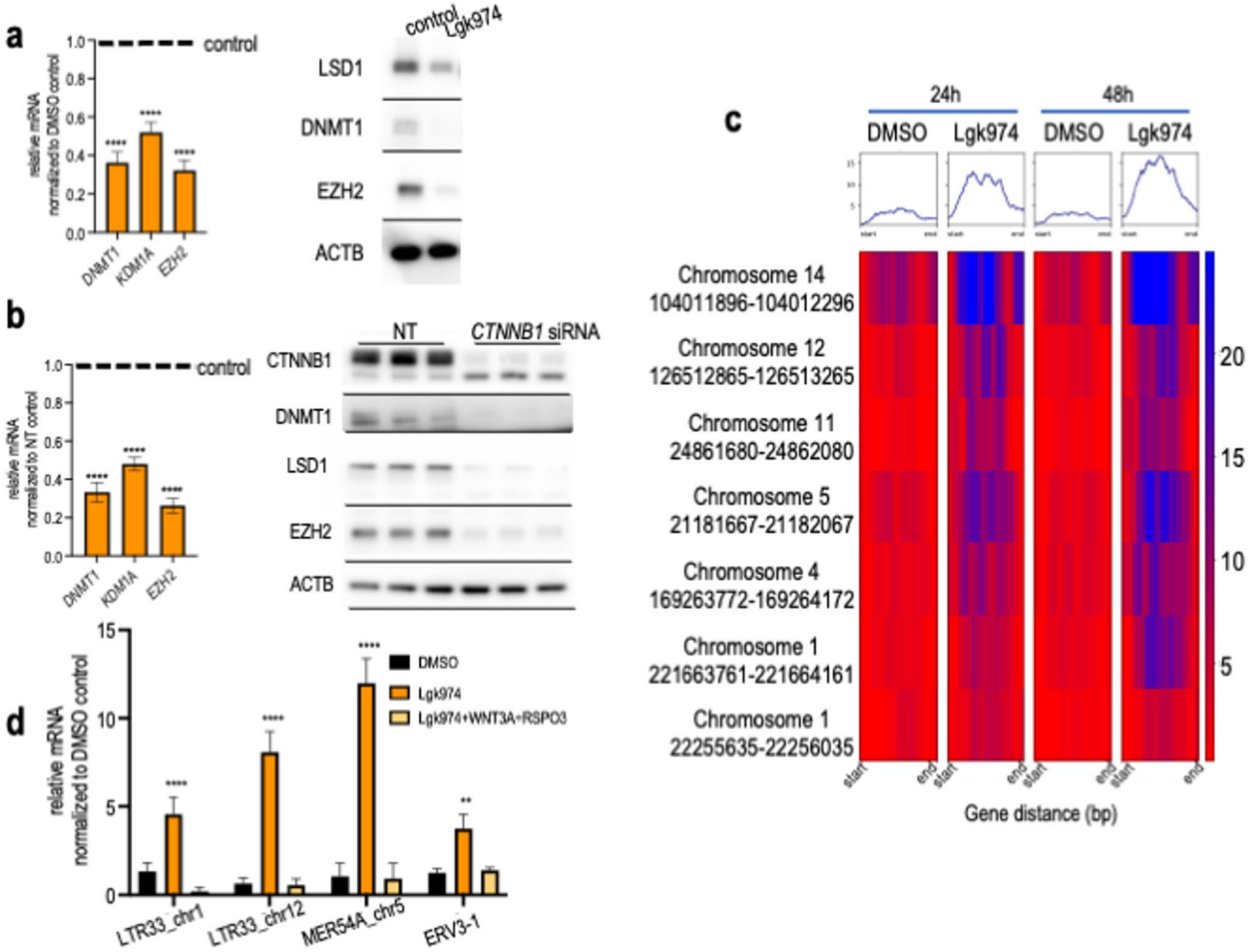

Fig. 6. Inhibition of WNT signaling results in decreased expression of epigenetic repressors and re-expression of endogenous retroviruses. (**a**) Western blot and quantitative PCR of epigenetic modulators from HPAF-II cells treated with Lgk974 for 48 h. The mRNA levels in control cells treated with vehicle were assigned a value of 1 (dashed line on graph). (**b**) Western blot and quantitative PCR of epigenetic modulators from HPAF-II cells treated with non-targeting (NT) or *CTNNB1* siRNA for 48 h. The mRNA levels in control cells treated with NT siRNA were assigned a value of 1 (dashed line on graph). (**c**) Heatmap showing the number and position (relative to transcriptional start and end sites of the nearest gene) of transposon insertion events at seven differentially accessible ERV-containing regions identified by ATAC-seq of HPAF-II cells treated with Lgk974 or vehicle control for 24–48 h ($n = 4$). (**d**) Quantitative PCR of select ERVs mapped to ERV-containing regions from HPAF-II cells treated with Lgk974 alone or together with exogenous WNT3a and RSPO3 for 48 h. (Two-way ANOVA with Fisher's least significant difference test versus control; * < 0.05, ** < 0.01, *** < 0.001, **** < 0.0001) $n = 3$.

ERV-containing regions at 24 and 48 h of treatment. This increased accessibility at ERV sites following inhibition of WNT is consistent with a model in which WNT pathway inhibition drives ERV re-expression.

To validate whether increased accessibility at ERV loci leads to their re-expression, we sought to detect transcripts of ERVs that were accessible in the ATAC-seq experiment at both 24 and 48 h following Lgk974 treatment and that appear in multiple ERV databases (Supplemental Table 1). Primers were designed to be unique to individual ERVs and to anneal completely within the ERV region identified (Supplemental Fig. 7c). HPAF-II cells were treated with Lgk974 alone or in combination with WNT3A and RSPO3 for 48 h and RNA samples were subjected to quantitative PCR. As shown in Fig. 6d, expression of these ERVs was significantly increased following Lgk974 treatment. Additionally, this upregulation was reversed by the addition of exogenous WNT3A and RSPO3, as we observed with ISGs. These results support a model in which inhibition of WNT signaling results in downregulation of epigenetic repressors, which induces re-expression of ERVs and generation of dsRNA.

To identify transcription factors that promote ERV expression following blockade of WNT signaling, a motif analysis was performed to identify the transcription factor binding sites located in regions of accessible chromatin. Given that HPAF-II cells have high basal WNT signaling, the predominant accessible motifs identified in vehicle-treated control cells were those of transcription factors in the WNT pathway, including LEF1, TCF3,

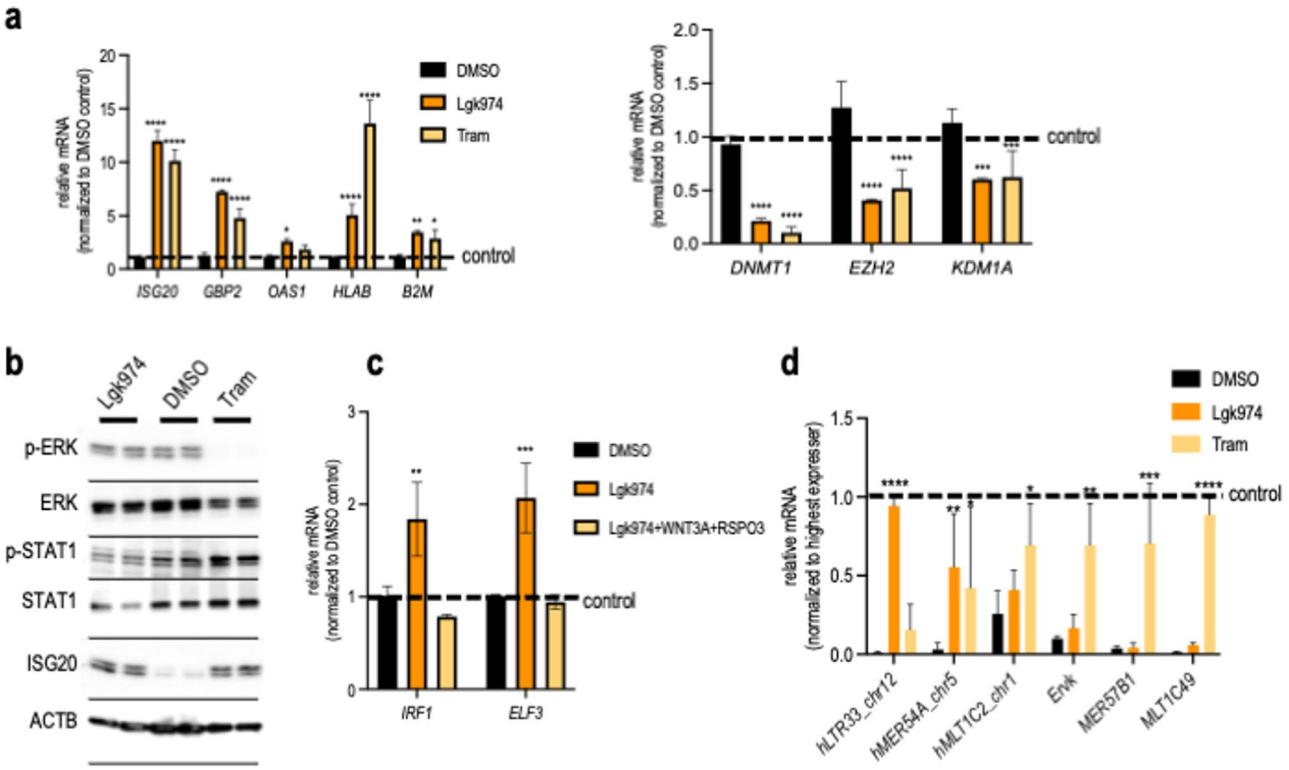

Fig. 7. Inhibition of WNT signaling induces ERV and ISG expression without modulating MEK/ERK signaling in HPAF-II cells. (**a**) Quantitative PCR of ISGs and epigenetic repressors from HPAF-II cells treated with Lgk974 or the MEK inhibitor trametinib for 48 h. The mRNA levels in control cells treated with vehicle were assigned a value of 1 (dashed line on graph). (**b**) Western blot from HPAF-II cells treated with Lgk974 or trametinib for 48 h. (**c**) Quantitative PCR data showing normalized mRNA levels of *IRF1* and *ELF3* in HPAF-II cells treated with Lgk974 alone or along with exogenous WNT3a and RSPO2 for 48 h. The mRNA levels in the vehicle-treated control cells were assigned a value of 1 (dashed line on graph), $n = 3$. (**d**) Quantitative PCR data showing normalized mRNA levels of ERVs identified by ATAC-seq and from [28] in HPAF-II cells treated with Lgk974 or trametinib for 48 h. The mRNA level of the highest expressing sample was assigned a value of 1 for ease of visualization, $n = 3$. (Two-way ANOVA with Fisher's least significant difference test versus control; * < 0.05, ** < 0.01, *** < 0.001, **** < 0.0001).

TCF4, and TCF7 (Supplemental Fig. 8). Analysis of the Lgk974 treated HPAF-II cells revealed the top motifs as binding sites for several members of the E74-like factor (ELF) subfamily of ETS transcription factors: ELF3, ELF4, and ELF5 (Supplemental Fig. 8). After 24 h of WNT pathway inhibition, ELF3 and ELF4 binding motifs were identified in 40-50% of regions of accessible chromatin. RNAseq data show modest upregulation of some of these transcription factors upon WNT inhibition (Supplemental Fig. 7d). Given that ELF transcription factors have diverse roles in the regulation of immune responses and immune cell differentiation, including modulation of interferon expression and function, this may implicate them in re-expression of ERVs or induction of ISGs[24–27].

Inhibition of WNT signaling induces ERV and ISG expression without modulating MEK/ERK signaling

Interestingly, a recent report found that inhibition of MEK1/2 (MAP kinase pathway) in pancreatic ductal adenocarcinoma cells induces ERV expression and a type-I interferon response, including in HPAF-II cells[28]. The mechanism put forth by Cortesi et al. is that MEK1/2 inhibition induces expression of ELF3, which then binds and induces expression of ERVs in accessible chromatin regions. The PRR involved is not identified and the model does not include loss of epigenetic repression. This ERV expression then triggers a feed-forward loop whereby IRF1 is induced and further drives expression of ERVs.

To compare the mechanisms through which MEK1/2 inhibition and WNT pathway inhibition result in increased ERV and ISG expression in WNT-driven cancer cells, HPAF-II cells were treated with MEK inhibitor trametinib or porcupine inhibitor Lgk974 for 48 h and analyzed for expression of ISGs, epigenetic repressors, and ERVs.

Overall, our data show largely similar responses to inhibition of these pathways with both trametinib and Lgk974 promoting downregulation of epigenetic repressors and increased expression of ISGs (Fig. 7a, Supplemental Fig. 9). However, Cortesi et al. show that trametinib induces IFNB expression and triggers STAT1 phosphorylation in pancreatic cancer cells, indicating a ligand-dependent induction of ISGs. In contrast, Lgk974 acts via a ligand-independent mechanism and does not induce interferon ligands or phosphorylation of

STAT1 (Fig. 4b). In addition, Lgk974, in contrast to trametinib, has no effect on ERK phosphorylation (Fig. 7b), indicating that blockade of WNT and MEK induce ERVs/ISGs by distinct molecular mechanisms. Despite this difference in signaling, levels of both ELF3 and IRF1 are elevated in HPAF-II cells following WNT inhibition (Fig. 7c), as Cortesi et al. reported for MEK1/2 inhibition, leaving open the possibility that ELF3 can activate IRF1 and create a similar feed-forward mechanism as was reported.

Comparing ERVs induced by trametinib versus Lgk974 shows that there is overlap. As seen in Fig. 7d, nearly all ERVs tested were induced by both MEK and WNT inhibition, but to varying degrees. Thus, it is possible that the mechanisms downstream of MEK1/2 and WNT inhibition ultimately converge on ELF3 to induce ERV re-expression. Given the importance of interferon signaling to innate cellular immunity, it is not surprising that multiple mechanisms can trigger this response.

Conclusions

This is the first report showing that inhibition of WNT signaling can induce expression of ISGs. The viral mimicry-type mechanism we identify for ISG expression differs from mechanisms described in other studies that have linked mitogenic RAS/RAF/MEK/ERK signaling with suppression of interferon signaling and/or ISG expression[15–17,28–40]. The mechanism we propose for induction of ISG expression following WNT pathway inhibition does not involve inhibition of RAS/RAF/MEK/ERK signaling. Using porcupine inhibitors or *CTNNB1* siRNA to block WNT signaling, we uncovered a robust, IFN ligand-independent induction of ISG expression in a broad range of human tumor cell lines harboring WNT pathway mutations. Our data suggest that in WNT mutant cancers, WNT signaling promotes epigenetic silencing of ERVs, keeping the dsRNA sensing pathways off and suppressing basal ISG expression. WNT pathway blockade results in decreased expression of epigenetic repressors (DNMT1, EZH2, KDM1A), allowing re-expression of ERVs, generation of dsRNA, activation of the RIGI/MDA5 dsRNA sensing pathway and finally induction of ISG expression (Supplemental Fig. 10).

Since ISGs may enhance anti-tumor immunity (for example, by stimulating antigen processing and presentation by tumor cells), our data suggest that blockade of WNT signaling in WNT-driven tumors might sensitize them to immunotherapy. However, targeting the WNT pathway in the clinic has long been a challenge due to the existence of multiple ligands/receptors as well as serious on-target toxicities. Currently, there are no WNT-targeted therapies approved[41]. The mechanism outlined in this study may offer a workaround to target the downstream mechanisms by which WNT promotes immune evasion. Several human tumor lines included in this study (e.g., HPAF-II, HepG2) have intact interferon signaling that can be exploited to induce ISG expression despite active WNT signaling. There are also several epigenetic therapies currently approved that induce viral mimicry as a mechanism of activating ISGs[42].

Given the complexity of WNT signaling, it is highly unlikely that the mechanism we identify here, repression of the type-I interferon system, is the sole way that WNT drives immune evasion. Indeed, our initial hypothesis-generating RNA-seq experiment identified a broad range of cytokines and chemokines upregulated by WNT inhibition (Supplemental Fig. 1, 2). In addition, given that both inhibition of WNT and inhibition of MEK1/2 can induce ISGs in HPAF-II cells, other signaling pathways may play an additive or synergistic role alongside WNT.

In closing, our data demonstrate a role for tumor cell WNT signaling in the suppression of ISG expression. This previously unappreciated mechanistic understanding of how WNT activation promotes immune evasion points to epigenetic modulators and tumor-targeted interferon ligands as potential clinical interventions that could sensitize WNT-driven tumors to immune checkpoint inhibition and convert non-T-cell inflamed/cold tumors to T-cell inflamed/hot tumors. The ability to target WNT-driven tumors with ICI therapeutics would greatly improve the utility of immunotherapies to the benefit of patients.

Materials and methods

Cell Culture

HPAF-II (ATCC® CRL1977™), Hep G2 (ATCC® HB-8065™), AsPC-1 (ATCC® CRL1682™), BT549 (ATCC® HTB-122™), Cal27 (ATCC® CRL-2095™), and J82 (ATCC® HTB-1™) were as recommended by ATCC. LIM1215 (Cell Bank Australia CBA-0161) were maintained in RPMI-1640 Medium with 10% FBS, 2mM L-Glutamine, 1x penicillin-streptomycin, 25mM HEPES, 0.6ug/mL Insulin, 1ug/mL Hydrocortisone, and 10 µm 1-Thioglycerol. JHOM2B (Riken Cell Bank RCB1682) was maintained in DMEM: F12 Medium supplemented with 10% FBS, 2mM L-Glutamine, 0.1mM non-essential amino acids, and 1x penicillin-streptomycin. PA-TU-8988 S (DSMZ ACC 204) were maintained in Dulbecco's Modified Eagle's Medium supplemented with 5% heat inactivated FBS, 5% horse serum, 2mM L-Glutamine, and 1x penicillin-streptomycin. All cells were maintained in complete growth media at 37 C under 5% CO2 in a humid environment.

Bulk RNA-seq

mRNA-seq libraries were generated using KAPA® mRNA HyperPrep Kit (Roche Sequencing.) The starting material was 500 ng total RNA and fragmentation was done at 85 °C for 6 min. cDNA was ligated with 1.5 µM xGen Dual Index UMI Adapters (Integrated DNA Technologies) and amplified using 12 PCR cycles. Sequencing of the resulting libraries was done on the Illumina HiSeq 2500 platform using a 33 cycle, single-end sequencing recipe.

For RNA-seq data, the raw sequencing reads were processed through Omicsoft RNA-seq pipeline. Reads were quality checked and aligned to the Human reference genome B37 using Omicsoft aligner. Read counts for each gene were assigned by RSEM (RNA-Seq by Expectation Maximization) algorithm; only reads fully aligned (read start to end) to a gene/transcript are counted. Differential expression analysis was performed using the

DESeq2 package in R. DESeq2 and genes with an adjusted p-value < 0.01 and $|\log_2$ fold change$| > \log_2(1.5)$ were considered as differentially expressed.

Genes were ranked based on their differential expression statistics with log2 fold change values obtained from the DESeq2 analysis used for ranking. Genes with higher absolute log2 fold change values were ranked higher. Gene Ontology (GO) enrichment and pathway analysis were performed using the fgsea package in R. The ranked gene list was used as the input. The GO gene sets for the analysis were obtained from the Molecular Signatures Database (MSigDB). fsea was run for each differentially expressed gene set from each comparison. Top up and down enriched pathways were identified based on their normalized enrichment score (NES) with adjusted p-value < 0.01 and they were plotted with corresponding NES.

Western Blot

Protein lysates from cells were extracted in cold RIPA Lysis and Extraction Buffer combined with 1X Halt™ Protease and Phosphatase Inhibitor Cocktail (Thermo Fisher Scientific 78440). For Western Blot analysis, protein quantification was determined by BCA assay and lysate was combined with reducing 6X Laemmli SDS sample buffer and ran on a Novex™4–20% Tris Glycine gel (Invitrogen) in SDS-PAGE. Antibodies against c-Myc (5605), CDK4 (12790), CDK2 (18048), ISG20 (79004), OAS1(4498),CTNNB1(9562), phospho-Stat1 (9167), Stat1(9172), ISG15(2758), GBP2 (53311), phospho-TBK1/NAK (5483), TBK1/NAK (3504), phospho-IRF-3 (37829), MDA-5 (5321), RIG-I (3743), P-STING (19781),STING (13647), LSD1 (2184), DNMT1 (5032), EZH2 (5246), ERK (4695), phospho-ERK (4370) were purchased from Cell Signaling Technologies and used at 1:500 in 1% milk. Primary antibody against Axin2 (ab109307), GBP2 (ab179829), and IRF3 (ab68481) was purchased from Abcam and used at 1:500 in 1% milk. Anti-β-Actin antibody (Sigma A5316) used at 1:2000 in 1% milk. Chemiluminescence was detected on the Azure digital imager c300. Western blots were quantified with ImageJ Version 2.14.0/1.54 f.

In vitro assays

HPAF-II, PATU8988S and ASPC1 cells were treated with 1 μm LGK-974 (StemRD L974-002) and 10nM ETC-159 (MedChemExpress HY-18988) 72 h after seeding 20,000 cells/well in 6-well plate and lysed 24–48 h after treatment. As a control, dimethylsulfoxide(DMSO) was added to cells in the same volume used for LGK-974 and ETC-159. Five independent samples for each treatment group were analyzed for molecular profiling. CAL27, J82, HPAF-II and BT 549 cells were treated with 1000ng recombinant human Wnt-3a (R&D 5036-WN-010/CF) and 100ng recombinant human R-spondin 3 protein (R&D 3500-RS-025/CF) or 100ng recombinant human R-spondin 2 protein (R&D 3266-RS-025/CF) 72 h after seeding 100,000 cell/well in 6-well plate and lysed 48 h after treatment.

HPAF-II cells were treated with 20ug/ml IFNRA1 function blocking antibody, 500pM recombinant human IFN-alpha2b protein (R&D 11013-IF), 1 nM human IFN-gamma protein (R&D 285-IF), 1 μm LGK-974, and/or 5 μM ruxolitinib (Tocris Bioscience 7064/50) 48 h after seeding 120,000 cells/well in a 6-well plate and lysed 1–48 h post- treatment as described.

HPAF-II cells were treated with 20nM Tramitinib (Selleckchem GSK1120212) 48 h after plating 120,000 cells/well in a 6-well plate and lysed 48 h post- treatment.

siRNA knockdown

SMARTpool ON-TARGETplus Human siRNA was used to knock down target of interest in human cell lines using reverse transfection with Lipofectamine™ RNAiMAX Transfection Reagent (Thermo Fisher Scientific 13778150) according to manufacturer's protocol with ON-TARGETplus Non-targeting Control Pool (Horizon Discovery Ltd. D-001810-10-20) and untreated cells as a control. To each well of a 6-well plate, 24pmol of siRNA duplex-Lipofectamine RNAimax complex was added in serum and antibiotic free cell media. After 15 min at room temperature, cells were seeded at 120,000 cells/well in antibiotic free media. Cells were lysed 72 h after siRNA knockdown. Multiple wells per condition served as independent replicates. siRNAs used *CTNNB1* (Horizon Discovery Ltd. L-003482-00-0020), *DDX58 (RIG-I)* (Horizon Discovery Ltd. L-012511-00-020), *IFIH1 (MDA-5)* (Horizon Discovery Ltd. L-013041-00-0020), *TMEM173(STING)* (Horizon Discovery Ltd. L-024333-00-020), *MYC* (Horizon Discovery Ltd. L-003282-02-0020).

Poly (I: C) (LMW) dsRNA (Invivogen tlrl-picw) was transfected at 2ug/ml using Lipofectamine™ 3000 (Invitrogen™ L3000001) according to manufacturer's protocol in HPAF II cells seeded one day prior at 20,000 cells per well in a 6 well plate and lysed after 1, 2, and 3 h. Poly dA: dT naked dsDNA (Invivogen tlrl-patn) was transfected for 4 h at 2ug/ml using Lipofectamine™ 3000 (Invitrogen™ L3000001) according to manufacturer's protocol in HPAF II cells 48 h post *TMEM173(STING)* siRNA knockdown.

Quantitative PCR

TRIzol™ Reagent (Invitrogen 15596026) was used to lyse the cells and isolate RNA. Total RNA was purified using MagMAX™-96 for Microarrays Total RNA Isolation Kit (Ambion by Life Technologies) according to manufacturer's specifications. Genomic DNA was removed using RNase-Free DNase Set (Qiagen).

mRNA (Up to 2.5ug) was reverse-transcribed into cDNA using SuperScript® VILO™ Master Mix (Invitrogen by Life Technologies) and Veriti 96-well PCR Thermal Cycler (Thermo Fisher Scientific). cDNA was amplified with the SensiFAST Probe Lo-ROX (Meridian) using the 12k Flex System (Applied Biosystems). PCR reactions were done in triplicate. Beta-actin was used to normalize cDNA input differences. Data reported as comparative CT method using delta delta CT. Probes described in Supplemental Materials.

Bulk ATAC-seq library preparation and sequencing

For ATAC-seq of pancreatic cancer cell line (HAPF-II), samples were processed using the Active Motif ATAC-Seq kit following the vendor provided protocol (ActiveMotif). Sequencing was performed on an Illumina Nextseq500 using R1 = 50 bp, R2 = 50 bp, I1 = 8 bp and I2 = 8 bp. To identify locations of putative ERVs, the databases HOMER, ERVmap, gEVE, HERVd, and EnHERV were used[43–47] For more details see Supplemental Materials and Methods.

ERV assay design

We used the chromosome location and nearest gene information provided by a previous next generation sequencing screen to query the HERVd database "Entities". Once an ERV was identified we used the annotated gene location in HERVd to retrieve the sequence from the GRCh38.p14 Primary Assembly in the NCBI Nucleotide database[2]. Assays (primers and probe) were designed to target each region.

Data availability

RNAseq data are available in supplemental file. TheATACseq datasets generated and analyzed during he current study are available inthe Gene Expression Omnibus (GEO), ascension number GSE309663. https://www.ncbi.nlm.nih.gov/geo/query/acc.cgi?acc=GSE309663__;!!ODpDvJZr5w!He6iXSFys_nyT_OfWHZ40qoi0faUaRfZ1E5XGMJsk6pVod7aGAQ3nhrBUSQXrGsXTaTPA6swt8dRwd1St1KH1jmttmg$Enter token yjgzcgwqvxobhmj.

Received: 30 September 2025; Accepted: 17 February 2026
Published online: 05 March 2026

References

1. Haslam, A. & Prasad, V. Estimation of the percentage of US patients with cancer who are eligible for and respond to checkpoint inhibitor immunotherapy drugs. *JAMA Netw. Open.* **2**, e192535. https://doi.org/10.1001/jamanetworkopen.2019.2535 (2019).
2. Grasso, C. S. et al. Genetic mechanisms of immune evasion in colorectal cancer. *Cancer Discov.* **8**, 730–749. https://doi.org/10.1158/2159-8290.CD-17-1327 (2018).
3. Harding, J. J. et al. Prospective genotyping of hepatocellular carcinoma: Clinical implications of next-generation sequencing for matching patients to targeted and immune therapies. *Clin. Cancer Res.* **25**, 2116–2126. https://doi.org/10.1158/1078-0432.CCR-18-2293 (2019).
4. Luke, J. J., Bao, R., Sweis, R. F., Spranger, S. & Gajewski, T. F. <article-title update="modified" original="WNT/beta-catenin Pathway Activation Correlates with Immune Exclusion across Human Cancers">WNT/β-catenin pathway activation correlates with immune exclusion across human cancers. *Clin. Cancer Res.* **25**, 3074–3083. https://doi.org/10.1158/1078-0432.CCR-18-1942 (2019).
5. Sia, D. et al. Identification of an immune-specific class of hepatocellular carcinoma, based on molecular features. *Gastroenterology* **153**, 812–826. https://doi.org/10.1053/j.gastro.2017.06.007 (2017).
6. Xue, J. et al. Intrinsic beta-catenin signaling suppresses CD8(+) T-cell infiltration in colorectal cancer. *Biomed. Pharmacother.* **115**, 108921. https://doi.org/10.1016/j.biopha.2019.108921 (2019).
7. Casey, S. C. et al. MYC regulates the antitumor immune response through CD47 and PD-L1. *Science* **352**, 227–231. https://doi.org/10.1126/science.aac9935 (2016).
8. Spranger, S., Bao, R. & Gajewski, T. F. Melanoma-intrinsic beta-catenin signalling prevents anti-tumour immunity. *Nature* **523**, 231–235. https://doi.org/10.1038/nature14404 (2015).
9. Pilard, C. et al. Cancer immunotherapy: It's time to better predict patients' response. *Br. J. Cancer* **125**, 927–938. https://doi.org/10.1038/s41416-021-01413-x (2021).
10. Loh, K. M., van Amerongen, R. & Nusse, R. Generating cellular diversity and spatial form: Wnt signaling and the evolution of multicellular animals. *Dev. Cell* **38**, 643–655. https://doi.org/10.1016/j.devcel.2016.08.011 (2016).
11. Yu, R., Zhu, B. & Chen, D. Type I interferon-mediated tumor immunity and its role in immunotherapy. *Cell. Mol. Life Sci.* **79**, 191. https://doi.org/10.1007/s00018-022-04219-z (2022).
12. Marron, T. U. et al. Neoadjuvant cemiplimab for resectable hepatocellular carcinoma: A single-arm, open-label, phase 2 trial. *Lancet Gastroenterol. Hepatol.* **7**, 219–229. https://doi.org/10.1016/S2468-1253(21)00385-X (2022).
13. Bai, M. et al. The crosstalk between beta-catenin signaling and type I, type II and type III interferons in lung cancer cells. *Am J Transl Res* **9**, 2788–2797 (2017).
14. Baril, M. et al. Genome-wide RNAi screen reveals a new role of a WNT/CTNNB1 signaling pathway as negative regulator of virus-induced innate immune responses. *PLoS Pathog.* **9**, e1003416. https://doi.org/10.1371/journal.ppat.1003416 (2013).
15. Zimmerli, D. et al. MYC promotes immune-suppression in triple-negative breast cancer via inhibition of interferon signaling. *Nat. Commun.* **13**, 6579. https://doi.org/10.1038/s41467-022-34000-6 (2022).
16. Krenz, B. et al. MYC- and MIZ1-dependent vesicular transport of double-strand RNA controls immune evasion in pancreatic ductal adenocarcinoma. *Cancer Res.* **81**, 4242–4256. https://doi.org/10.1158/0008-5472.CAN-21-1677 (2021).
17. Muthalagu, N. et al. Repression of the type I interferon pathway underlies MYC- and KRAS-dependent evasion of NK and B cells in pancreatic ductal adenocarcinoma. *Cancer Discov.* **10**, 872–887. https://doi.org/10.1158/2159-8290.CD-19-0620 (2020).
18. Alberts, R. et al. Genetic association analysis identifies variants associated with disease progression in primary sclerosing cholangitis. *Gut* **67**, 1517–1524. https://doi.org/10.1136/gutjnl-2016-313598 (2018).
19. Huang, W. et al. Dual inhibitors of DNMT and HDAC induce viral mimicry to induce antitumour immunity in breast cancer. *Cell Death Discov.* **10**, 143. https://doi.org/10.1038/s41420-024-01895-7 (2024).
20. Kim, S. J., Kiser, P. K., Asfaha, S., DeKoter, R. P. & Dick, F. A. EZH2 inhibition stimulates repetitive element expression and viral mimicry in resting splenic B cells. *EMBO J.* **42**, e114462. https://doi.org/10.15252/embj.2023114462 (2023).
21. Sheng, W. et al. LSD1 ablation stimulates anti-tumor immunity and enables checkpoint blockade. *Cell* **174**, 549-563 e519. https://doi.org/10.1016/j.cell.2018.05.052 (2018).
22. Schlesinger, S. & Meshorer, E. Open chromatin, epigenetic plasticity, and nuclear organization in pluripotency. *Dev. Cell* **48**, 135–150. https://doi.org/10.1016/j.devcel.2019.01.003 (2019).
23. May, D. et al. Live imaging reveals chromatin compaction transitions and dynamic transcriptional bursting during stem cell differentiation in vivo. *Elife* https://doi.org/10.7554/eLife.83444 (2023).
24. You, F. et al. ELF4 is critical for induction of type I interferon and the host antiviral response. *Nat. Immunol.* **14**, 1237–1246. https://doi.org/10.1038/ni.2756 (2013).
25. Suico, M. A., Shuto, T. & Kai, H. Roles and regulations of the ETS transcription factor ELF4/MEF. *J. Mol. Cell Biol.* **9**, 168–177. https://doi.org/10.1093/jmcb/mjw051 (2017).

26. Li, D. et al. IRF6 is directly regulated by ZEB1 and ELF3, and predicts a favorable prognosis in gastric cancer. *Front. Oncol.* **9**, 220. https://doi.org/10.3389/fonc.2019.00220 (2019).
27. Fung, K. Y. et al. Expression of interferon epsilon in mucosal epithelium is regulated by Elf3. *Mol. Cell Biol.* **44**, 334–343. https://doi.org/10.1080/10985549.2024.2366207 (2024).
28. Cortesi, A. et al. Activation of endogenous retroviruses and induction of viral mimicry by MEK1/2 inhibition in pancreatic cancer. *Sci. Adv.* **10**, eadk5386. https://doi.org/10.1126/sciadv.adk5386 (2024).
29. Elewaut, A. et al. Cancer cells impair monocyte-mediated T cell stimulation to evade immunity. *Nature* **637**, 716–725. https://doi.org/10.1038/s41586-024-08257-4 (2025).
30. Gong, K. et al. EGFR inhibition triggers an adaptive response by co-opting antiviral signaling pathways in lung cancer. *Nat. Cancer* **1**, 394–409. https://doi.org/10.1038/s43018-020-0048-0 (2020).
31. Gurule, N. J. et al. A tyrosine kinase inhibitor-induced interferon response positively associates with clinical response in EGFR-mutant lung cancer. *NPJ Precis. Oncol.* **5**, 41. https://doi.org/10.1038/s41698-021-00181-4 (2021).
32. Boumelha, J. et al. An immunogenic model of KRAS-mutant lung cancer enables evaluation of targeted therapy and immunotherapy combinations. *Cancer Res.* **82**, 3435–3448. https://doi.org/10.1158/0008-5472.CAN-22-0325 (2022).
33. Tian, J. et al. Combined PD-1, BRAF and MEK inhibition in BRAF(V600E) colorectal cancer: A phase 2 trial. *Nat. Med.* **29**, 458–466. https://doi.org/10.1038/s41591-022-02181-8 (2023).
34. Anastasiou, P. et al. Combining RAS(ON) G12C-selective inhibitor with SHP2 inhibition sensitises lung tumours to immune checkpoint blockade. *Nat. Commun.* **15**, 8146. https://doi.org/10.1038/s41467-024-52324-3 (2024).
35. Zhao, Y. et al. IDH1 mutation inhibits differentiation of astrocytes and glioma cells with low oxoglutarate dehydrogenase expression by disturbing α-ketoglutarate-related metabolism and epigenetic modification. *Life Metab.* **3**, loae002. https://doi.org/10.1093/lifemeta/loae002 (2024).
36. Bragelmann, J. et al. MAPK-pathway inhibition mediates inflammatory reprogramming and sensitizes tumors to targeted activation of innate immunity sensor RIG-I. *Nat. Commun.* **12**, 5505. https://doi.org/10.1038/s41467-021-25728-8 (2021).
37. Korpela, S. P. et al. Role of epidermal growth factor receptor inhibitor-induced interferon pathway signaling in the head and neck squamous cell carcinoma therapeutic response. *J. Transl. Med.* **19**, 43. https://doi.org/10.1186/s12967-021-02706-8 (2021).
38. Gureghian, V. et al. A multi-omics integrative approach unravels novel genes and pathways associated with senescence escape after targeted therapy in NRAS mutant melanoma. *Cancer Gene Ther.* **30**, 1330–1345. https://doi.org/10.1038/s41417-023-00640-z (2023).
39. Goel, S. et al. CDK4/6 inhibition triggers anti-tumour immunity. *Nature* **548**, 471–475. https://doi.org/10.1038/nature23465 (2017).
40. Adachi, Y. et al. Inhibition of FGFR reactivates IFNgamma signaling in tumor cells to enhance the combined antitumor activity of lenvatinib with anti-PD-1 antibodies. *Cancer Res.* **82**, 292–306. https://doi.org/10.1158/0008-5472.CAN-20-2426 (2022).
41. Park, W. J. & Kim, M. J. A new wave of targeting "undruggable" Wnt signaling for cancer therapy: Challenges and opportunities. *Cells* https://doi.org/10.3390/cells12081110 (2023).
42. Gavine, P. R. et al. AZD4547: An orally bioavailable, potent, and selective inhibitor of the fibroblast growth factor receptor tyrosine kinase family. *Cancer Res.* **72**, 2045–2056. https://doi.org/10.1158/0008-5472.CAN-11-3034 (2012).
43. Paces, J. et al. HERVd: The Human Endogenous RetroViruses Database: Update. *Nucleic Acids Res.* **32**, D50. https://doi.org/10.1093/nar/gkh075 (2004).
44. Paces, J., Pavlicek, A. & Paces, V. HERVd: Database of human endogenous retroviruses. *Nucleic Acids Res.* **30**, 205–206. https://doi.org/10.1093/nar/30.1.205 (2002).
45. Heinz, S. et al. Simple combinations of lineage-determining transcription factors prime cis-regulatory elements required for macrophage and B cell identities. *Mol. Cell* **38**, 576–589. https://doi.org/10.1016/j.molcel.2010.05.004 (2010).
46. Nakagawa, S. & Takahashi, M. U. gEVE: A genome-based endogenous viral element database provides comprehensive viral protein-coding sequences in mammalian genomes. *Database (Oxford)* https://doi.org/10.1093/database/baw087 (2016).
47. Tongyoo, P. et al. EnHERV: Enrichment analysis of specific human endogenous retrovirus patterns and their neighboring genes. *PLoS ONE* **12**, e0177119. https://doi.org/10.1371/journal.pone.0177119 (2017).

Acknowledgements

The authors wish to acknowledge the members of the Regeneron DNA Core, Tissue Culture Core, and Molecular Profiling Core.

Author contributions

CMW conceived and designed study, performed experiments, interpreted the results, prepared the manuscript draft. JHC performed experiments wrote and edited the manuscript draft. VRD performed ATAC-seq analysis, interpreted data, wrote and edited the manuscript draft. LJL performed RNAseq analysis. SN performed experiments wrote and edited the manuscript draft. HC performed experiments. WW performed RNAseq analysis. RS and CA performed ATAC-seq. DA designed ERV primers for validation. NTG assisted with RNAseq and ATACseq study design and interpretation, gave intellectual comments. CD contributed to conception and design of this study and interpretation of results and edited the manuscript with critical intellectual input. All authors contributed to the article and approved the submission.

Declarations

Competing interests

The authors declare no competing interests.

Additional information

Supplementary Information The online version contains supplementary material available at https://doi.org/10.1038/s41598-026-40894-9.

Correspondence and requests for materials should be addressed to C.M.W.